Parameter dependence of the radial electric field in the edge pedestal of hydrogen, deuterium and helium plasmas

E. Viezzer, T. Pütterich, R. M. McDermott, G. D. Conway, M. Cavedon, M. G. Dunne, R. Dux, E. Wolfrum and the ASDEX Upgrade Team

Max-Planck-Institut für Plasmaphysik, EURATOM Association, Boltzmannstr. 2, 85748 Garching, Germany

E-mail: Eleonora.Viezzer@ipp.mpg.de

Abstract. The characteristics of the edge radial electric field (E_r) are studied in deuterium, hydrogen and helium plasmas at ASDEX Upgrade. The minimum of the E_r well is analyzed as a function of pedestal parameters and the best correlation is found between the depth of the E_r well and the ion pressure at the pedestal top. This result is consistent with E_r being balanced by the main ion pressure gradient term. Studying the radial position of the E_r minimum reveals that the E_r well moves closer to the last closed flux surface the deeper the E_r well is. This suggests that for deeper E_r wells the distance between the steepest gradients in the ion temperature and ion density profile is reduced. The width of the E_r well shows no significant variations despite changing the ion temperature, magnetic field and plasma particle species. At AUG, the E_r well is on average 1.2 cm wide. A multi-machine comparison supports a machine size scaling of E_r and indicates that the E_r shear layer covers the outer 2 % of the plasma minor radius independent of the size of the machine. Based on this scaling, the width of the E_r well in ITER is estimated to $\sim$4 cm.

PACS numbers: 52.55.Fa, 52.25.Vy, 52.30.-q, 52.70.-m

1. Introduction

Edge transport barriers (ETBs) are built up during the transition from a low (L-mode) to a high confinement regime (H-mode) which is characterized by reduced turbulence and transport [1]. The formation of the ETB is strongly connected to the existence of a sheared plasma flow perpendicular to the magnetic field caused by a local radial electric field E_r. The strong gradients in E_r and the associated $\mathbf{E}\times\mathbf{B}$ velocity shear play a fundamental role in edge turbulence suppression, transport barrier formation and the transition to the H-mode [2]. Since the structure of the ETB sets boundary conditions for the heat and particle transport in the plasma core it is essential to understand the underlying mechanism that is responsible for the edge pedestal.
Spatially and temporally resolved measurements of E_r in various tokamaks [3, 4, 5, 6,

7, 8] showed that at the H-mode transition the edge E_r well becomes more negative and a strong E_r shear develops that is accompanied by a strong reduction in the turbulent fluctuations. Though the importance of E_r was already acknowledged 25 years ago [9, 2, 10] the understanding of the interplay between $\mathbf{E}\times\mathbf{B}$ shearing, turbulence and transport reduction, pedestal formation and confinement improvement is still not completely elucidated. As of yet, no theory can quantitatively predict the spatial structure (including the depth and the width) of the E_r well. A better understanding of the parameter dependencies of the edge radial electric field can contribute to gain better knowledge of the pedestal physics.

The characteristics of the depth and the spatial extent of the E_r well were investigated in the ETB of hydrogen, deuterium and helium plasmas at ASDEX Upgrade (AUG). The structure of the E_r well is studied as a function of the pedestal height and correlations to the Larmor radius are analyzed. This paper is organized as follows: section 2 briefly describes the diagnostic technique used in this paper. In section 3 the interconnections between E_r and pedestal parameters are discussed while in section 4 possible dependencies of the width of the E_r well are examined. In section 5 a summary and discussion are given.

2. Diagnostic technique

At AUG, the radial electric field is diagnosed via Doppler reflectometry [11] and spectroscopically via a combination of poloidal and toroidal active charge exchange recombination spectroscopy (CXRS) diagnostics [12]. Using an external source of neutral particles, such as a neutral beam, has the advantage of spatial localization as the measured active charge exchange signal is localized in the volume where the lines of sight of the CXRS diagnostics intersect the path of the neutral beam particles. The radial electric field can be evaluated directly from the CXRS measurements via the radial force balance equation [10] since all quantities of the ion species (temperature T_α, density n_α and poloidal and toroidal rotation velocity, $v_{\theta,\alpha}$ and $v_{\phi,\alpha}$, of the species α) are determined from the measured spectra [13]. At AUG, the CXRS systems typically utilize the B^{5+} ($n = 7 \rightarrow 6$) CX line at 494.467 nm. However, CXRS measurements have also been performed on He, C, N, Ne and Ar.

In this work, the localization of the E_r dip is of very high quality and has small uncertainties (2-3 mm) due to two aspects: First, the measurements are fixed in real space and have a resolution between 3 and 5 mm. Secondly, the ion temperature profile is part of the CXRS measurements and is therefore rigidly aligned to the E_r profile. The relative alignment of E_r to the electron profiles and the separatrix position follows an established scheme [8] that makes use of the unique edge diagnostic capabilities available at AUG. Here, the CXRS measurements are aligned relatively to the electron measurements assuming that the radial position of the steepest gradients in the electron (T_e) and ion temperature (T_i) profile coincides [8]. This assumption is valid in the collisionality regime in which a sufficient coupling between electrons and ions is provided

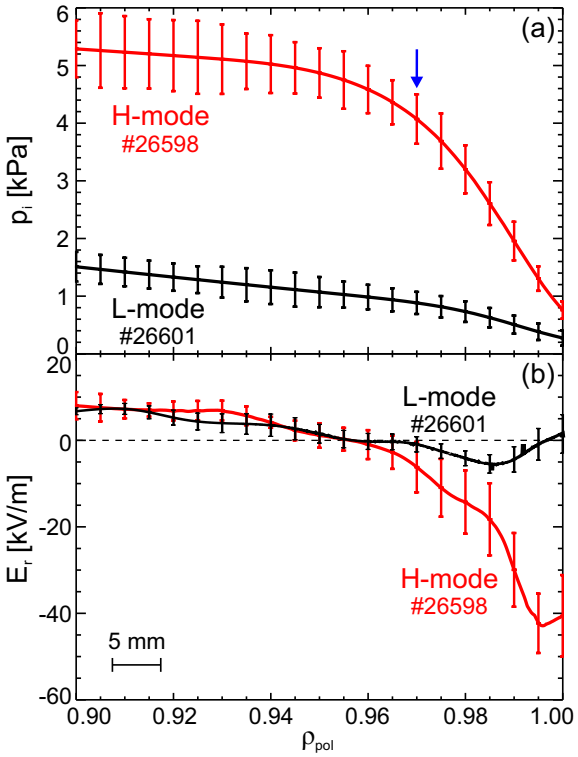

Figure 1: (a) Ion pressure, p_i, and (b) radial electric field, E_r, profile in L-mode (black) and H-mode (red).

such that $T_e \approx T_i$ [14]. This also allows for an alignment with respect to the separatrix position, since the location of the separatrix is connected to T_e based on power balance and parallel heat transport studies using a 1D heat conduction model [15]. As a result, all E_r profiles are reproducibly aligned [8].

Figure 1 shows example profiles of (a) the ion pressure p_i and (b) E_r measured in an L-mode (black) and an H-mode (red) discharge. The ion pressure is calculated using the measured T_i profile and assuming a radially varying dilution for the ion density profile, $n_i = n_e(1 - \sum_\alpha Z_\alpha c_\alpha)$, where n_e is the measured electron density profile, Z_α the impurity charge state and c_α the impurity concentration as measured with CXRS. It should be noted that the profiles used for the analysis presented here are fitted with a spline function. In this paper following convention is used to study the connection between E_r and the edge transport barrier: the pedestal top is defined at the radial position $\rho_{pol} = 0.97$ (marked by a blue arrow in figure 1(a)). The minimum of E_r corresponds to the deepest value of the E_r well. The width of the E_r well is defined as the full width at half maximum (FWHM); here, the half width at half maximum is determined from the measured profile and then multiplied by 2 to obtain the FWHM.

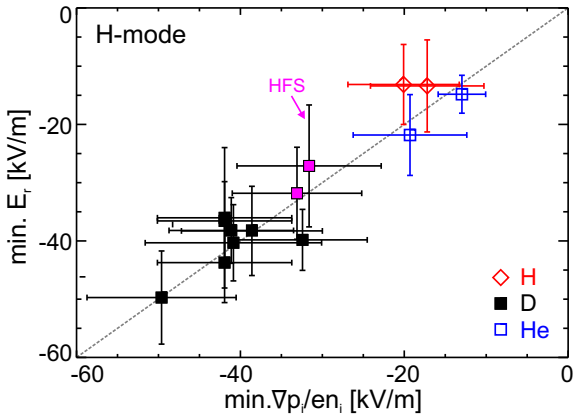

Figure 2: Depth of the E_r well versus minimum of the main ion pressure gradient term $\nabla p_i/en_i$ measured in hydrogen (red diamonds), deuterium (black squares) and helium (blue open squares) plasmas. The discharge that includes LFS and HFS measurements is highlighted in magenta.

3. Interdependencies between E_r and pedestal parameters

Recent AUG results [8] showed that in H-mode the radial electric field E_r is in balance with the main ion pressure gradient term $\nabla p_i/en_i$, similar to observations on Alcator C-Mod [6]. This demonstrates that E_r and the gradients of the main ion species are intimately connected and is in keeping with the neoclassical nature of E_r in the edge pedestal [16, 17, 18, 19, 20]. This was recently corroborated by comparing the E_r data measured in the pedestal of highly collisional (plateau to Pfirsch-Schlüter regime) H-mode plasmas to various neoclassical models, which showed very good agreement in all cases [16].

Figure 2 shows the minimum of the E_r well plotted as a function of the minimum in the main ion pressure gradient term $\nabla p_i/en_i$ measured in the ETB of deuterium (D, black squares), hydrogen (H, red diamonds) and helium (He, blue open squares) plasmas. Independent of the plasma species, the radial electric field is balanced by the pressure gradient term of the main ions. It should be noted that in helium plasmas the main ion species is measured directly via CXRS on He^{2+} ($n = 4 \rightarrow 3$). In deuterium and hydrogen plasmas, the CXRS measurements are performed on impurity ions, such as B^{5+}, C^{6+} and N^{7+}, since main ion CXRS measurements on H and D are difficult to interpret due to the complexity of the spectra. In these discharges the plasma current, I_p, varied from 0.8 to 1.0 MA, the toroidal magnetic field B_ϕ from 2.3 to 2.6 T, the core line-averaged density from 5.8 to $10.7 \times 10^{19}\,\mathrm{m}^{-2}$ and the total heating power from 4.1 to 11.8 MW. The data are typically measured at the low-field side (LFS), since the LFS diagnostics are based on CXRS at a heating beam that is usually switched on to provide T_i and rotation measurements. New gas-puff CXRS diagnostics were recently installed at the high-field side (HFS) of AUG to study possible asymmetries on a flux surface [21, 22, 23]. It was found that the impurity density has a poloidal dependence

with an impurity accumulation at the HFS of up to a factor of ∼3, which in turn leads to asymmetric rotation profiles to maintain the condition of divergence-free flows on a flux surface [23, 24]. However, the presence of an impurity density asymmetry does not have a strong impact on the relationship between E_r and the main ion pressure gradient term. The discharge in which detailed CXRS measurements could be provided at both the HFS and LFS is highlighted in magenta in figure 2. Here, the HFS main ion pressure gradient term has been evaluated assuming that the electron density is constant on the flux surfaces. For the calculation of the HFS ion density the measured LFS electron density profile has been mapped to the HFS taking the measured impurity density at the HFS into account to calculate the radially varying dilution of the plasma. Note that the CXRS measurements at the HFS are aligned to the LFS profiles using the assumption that the ion temperature is constant on the flux surfaces [25, 23]. Comparing the main ion pressure gradient term evaluated at the HFS to the radial electric field derived from the HFS CXRS measurements shows good agreement despite the existence of a poloidal impurity density asymmetry.

Studying the relationship between the depth of the E_r well and the height of the edge transport barrier reveals that the minimum of E_r is correlated with the ion pressure at the pedestal top. Figure 3 shows the E_r minimum as a function of the (a) ion temperature $T_i^{ped,top}$, (b) ion density $n_i^{ped,top}$ and (c) ion pressure $p_i^{ped,top}$ at the top of the pedestal. For the evaluation of $n_i^{ped,top}$ the dilution due to the impurity concentration as measured with CXRS has been taken into account. The parameter range for the database shown in figure 3 is summarized in table 1. Here, the main ion collisionality $\nu_{*,i}$ is evaluated at the pedestal top ($\rho_{pol} = 0.97$) and corresponds to the effective collision frequency normalized to the bounce frequency of the trapped particles [26]. Data obtained in impurity seeded deuterium H-modes (here, nitrogen and neon) are

plasma species	H	D	He
I_p [MA]	0.8	0.6–1.0	1.0
B_ϕ [T]	2.6	2.3–2.5	2.5
$\bar{n}_e$ [10^{19} m^{-2}]	6.1–6.3	3.0–9.6	9.0–10.7
P_{heat} [MW]	7.2	1.0–11.8	9.6–10.2
$\nu_{*,i}^{ped,top}$	1.6–2.2 (Pl)	0.8–8.4 (B/Pl/PS)	11.2–11.5 (PS)
β_N	1.0	0.4–2.4	1.3–1.4
q_{95}	5.2	3.9–7.3	4.4

Table 1: Parameter range for the discharges shown in figure 3: plasma current I_p, toroidal magnetic field on-axis B_ϕ, core line-averaged density $\bar{n}_e$, total heating power P_{heat}, main ion collisionality at the pedestal top $\nu_{*,i}^{ped,top}$, normalized beta β_N which gives the ratio between the plasma pressure and the magnetic pressure, and the edge safety factor q_{95}. The collisionality regimes, i.e. banana (B), plateau (Pl) and Pfirsch-Schlüter regimes (PS), are also indicated in the table.

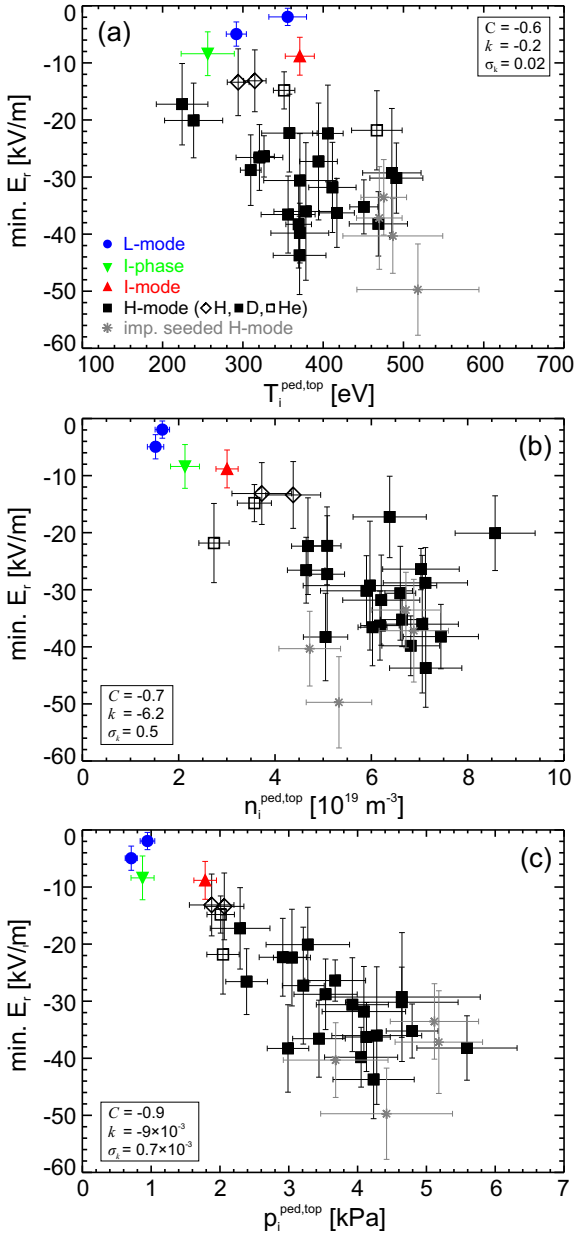

Figure 3: Depth of the E_r well as a function of the pedestal top ($\rho_{pol} = 0.97$) (a) ion temperature $T_i^{ped,top}$, (b) ion density $n_i^{ped,top}$ and (c) ion pressure $p_i^{ped,top}$. The correlation coefficient C, the slope k and its standard deviation σ_k of a linear least-squares fit to the data are quoted in each subfigure.

marked in grey, while an I-phase data point is highlighted in green. The I-phase [27] is an intermediate limit cycle phase, which typically precedes the L-H transition at low densities, and is characterized by an increase in the turbulence level across the whole plasma edge, which then starts to pulsate at 2–4 kHz. The data points measured in helium plasmas are marked with black open squares while hydrogen plasmas are highlighted with black open diamonds.

The lowest correlation is found between the minimum of the E_r well and the ion

temperature at the top of the pedestal. This is reflected by a smaller correlation factor C compared to the ion density and ion pressure (see figure 3). In addition, the slope k and its standard deviation σ_k of a linear least-squares approximation of the data are quoted in each subplot to indicate the goodness of the fit. A weak trend between deeper E_r wells and higher pedestal top ion densities is observed, however, within the H-mode data, the scatter is rather large and no clear correlation is found. The best correlation is found between the minimum of the E_r well and $p_i^{ped,top}$ (see figure 3(c)), which is corroborated by a high correlation factor of C = -0.9. In general, the E_r well is observed to be deeper for higher pedestal top pressures, which is consistent with the finding that E_r is in balance with the main ion pressure gradient term.

The energy confinement time of the plasma is correlated to the pedestal top pressure due to stiff T_i gradient scale lengths. Since the edge E_r profile behaves as expected from neoclassical theory [16] and the E_r well is mainly determined by the main ion pressure gradient term, the minimum of E_r, or the E_r shear, respectively, should show a dependence on the global plasma confinement. In figure 4 the maximum $\mathbf{E}\times\mathbf{B}$ shearing rate, defined as $\omega_{\mathbf{E}\times\mathbf{B}} = \frac{r}{q}\frac{\partial}{\partial r}(\frac{q}{r}\frac{E_r}{B})$ [28], is plotted against the global energy confinement factor $H_{98}(y,2)$. Moving from L- to H-mode the $\mathbf{E}\times\mathbf{B}$ shear becomes stronger, i.e. the E_r well deepens, and the energy confinement of the plasma increases. For the I-phase data

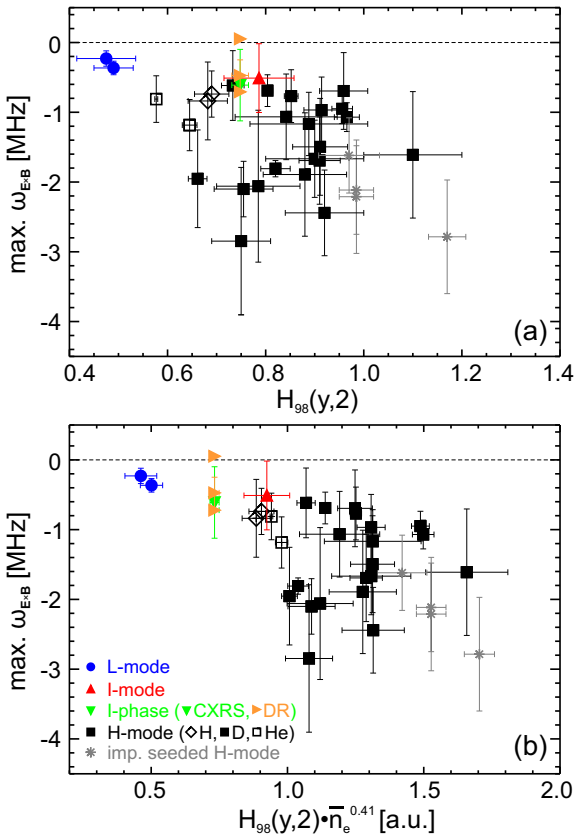

Figure 4: Maximum $\mathbf{E}\times\mathbf{B}$ shearing rate versus (a) energy confinement factor $H_{98}(y,2)$ and (b) $H_{98}(y,2)$ multiplied by the core line-averaged density $\bar{n}_e^{0.41}$.

point, three additional points are highlighted in orange (arrow symbols) which represent (from top to bottom) the minimum, the average and the maximum $\omega_{\mathbf{E}\times\mathbf{B}}$ as measured with Doppler reflectometry (DR) [29]. The characteristic pulsing of the turbulence in the I-phase affects the mean flow shear on the turbulence timescale ($\sim\mu$s) and a strong modulation of E_r, which is synchronized with the turbulence level, is observed [27]. The minimum and maximum $\omega_{\mathbf{E}\times\mathbf{B}}$ correspond to the minimum and maximum in the cyclic variation of E_r that is observed in the I-phase [27], while to reconstruct the average profile with DR each frequency step is averaged over a time period of 10 ms. The temporal resolution of the edge CXRS diagnostics (2.2 ms) [12] is too slow to resolve the cyclic variation of E_r, however, the average profile of the oscillations in E_r is measured by CXRS. Within the experimental uncertainties, good agreement in the average E_r shear as observed with CXRS and DR is obtained and the values lie in between the minimum and maximum $\mathbf{E}\times\mathbf{B}$ shearing rates.

As shown in figure 4(a) the scatter within the H-mode is substantial and only a weak correlation between the maximum $\mathbf{E}\times\mathbf{B}$ shear and H_{98}(y,2) is found. This points to a more complicated dependence between $\mathbf{E}\times\mathbf{B}$ shearing and improved plasma confinement, which has also been observed at JT-60U [30, 7]. Due to the density dependence of the τ_E(y,2)–scaling ($\propto \bar{n}_e^{0.41}$, $\bar{n}_e$ being the line-averaged electron density) the same $p_i^{ped,top}$ value can result in different H_{98}(y,2)–factors. This may explain the observation of strong $\mathbf{E}\times\mathbf{B}$ shearing rates, or higher pedestal top pressures, at lower energy confinement factors ($\sim$0.75, cf. figure 4(b)). These data points were measured in high density H-mode plasmas ($n_i^{ped,top} \sim 7\times10^{19}\,\mathrm{m}^{-3}$), where the τ_E(y,2)–scaling, which depends on the density, may not be valid [31]. A better correlation is found when multiplying the H_{98}(y,2) factor with the core line-averaged density $\bar{n}_e^{0.41}$ (see figure 4(b)), supporting that the τ_E(y,2)–scaling may not describe the data appropriately at very high densities.

In H-mode, the position of the minimum of the E_r well has been examined as a function of the distance to the location of the last closed flux surface. For deeper E_r wells the minimum appears to move towards the separatrix. This finding also suggests that the steepest gradients in the kinetic profiles should shift towards the separatrix. Note that this movement is observed in fully developed H-mode discharges and may be different when moving from L- to H-mode as reported in [32]. Figure 5 shows the distance of the minimum of E_r from the separatrix plotted against the depth of the E_r well. Here, only measurements from deuterium plasmas have been included in the analysis. The uncertainty of determining the position of the E_r minimum is given by the uncertainty of the radial profile alignment (2–3 mm, [8]). For two cases the radial distance of the minimum in the main ion pressure gradient term $\nabla p_i/n_i e$ was analyzed (marked by blue stars in figure 5), which shows the same trend. This supports that the radial alignment of the edge kinetic profiles is very accurate for the present work and is well suited to study effects on the mm range. The physical mechanism behind the radial movement remains, as yet, unclear as the relative positioning of both the density and temperature profiles and their gradients is crucial. However, for the two cases highlighted in blue in

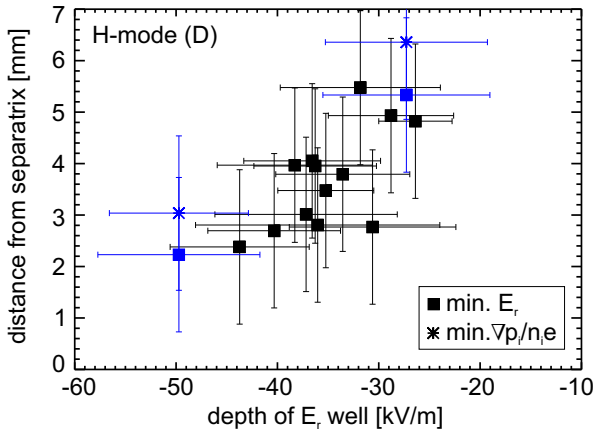

Figure 5: Distance of the E_r minimum from the separatrix versus depth of the E_r well measured in deuterium H-mode plasmas. The deepest and one of the more shallow E_r wells are highlighted in blue. The corresponding data points for the main ion pressure gradient term (i.e. the distance of the minimum in the main ion pressure gradient term from the separatrix) are marked by stars for the two cases shown in blue.

figure 5 the radial distance of $\nabla p_i/n_i e = (T_i \nabla n_i / n_i + \nabla T_i)/e$ from the separatrix was disentangled into the distance of $T_i \nabla n_i/n_i$ and ∇T_i. For these two data points the $T_i \nabla n_i/n_i$ term seems to move towards the separatrix, while the ∇T_i term stays close to the separatrix and does not move significantly. This indicates that for deeper E_r wells the radial distance between the steepest ∇n_i and ∇T_i decreases. This result is not unexpected since the pedestal widths for the electron temperature and density are observed to be different [33]. A statistical analysis including detailed edge profiles is needed to identify the mechanism responsible for this movement and will be performed in future studies.

4. E_r well width scaling

Comparing the E_r measurements from Alcator C-Mod [6], DIII-D [34, 35] and JET [4] showed that in H-mode the width of the E_r well scales with the size of the machine [6]. This relationship has also been examined at AUG using the E_r data from the new edge CXRS diagnostics. The data from fully developed H-mode discharges performed in deuterium, hydrogen and helium plasmas were included in the study. Figure 6(a) shows the width of the E_r well plotted against the depth of E_r. The uncertainty of the width determination is given by the radial resolution of the diagnostics (5 mm for the poloidal system [12]). Only small variations in the E_r well width are found, consistent with data from C-Mod [6]. On average the width is 1.2 cm with a standard deviation of 0.2 cm. This is also in quantitative agreement with measurements of the electron pedestal [14] which showed that the pedestal width of the electron pressure profile is $\sim$1.5 cm.
It should be noted that the definition of the E_r well width as stated in section 2 assumes symmetric E_r profiles. The half width at half maximum as determined from

the measured profiles (on average ∼6 mm) could be narrower than the diagnostic's capability to dissolve it. However, in case of asymmetric E_r wells, the width of E_r can still be discerned since the minimum width is ∼8 mm (half width at half maximum plus the minimal distance to the separatrix), which is beyond the spatial resolution of the instrument.

Figure 6(b) shows the E_r well width plotted as a function of the pedestal top toroidal

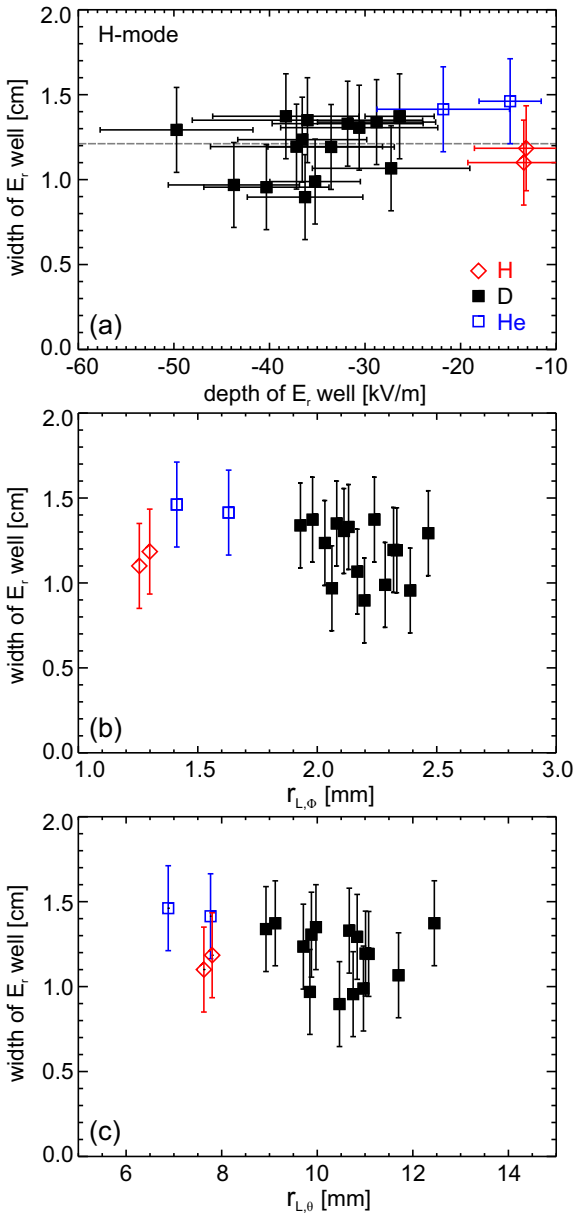

Figure 6: (a) Width versus depth of the E_r well in H-mode plasmas, E_r well width plotted as a function of the (b) toroidal ($r_{L,\phi}$) and (c) poloidal ($r_{L,\theta}$) Larmor radius at the pedestal top. Data measured in D plasmas are marked by black squares, while data obtained in H and He plasmas are highlighted by open diamonds and open squares, respectively.

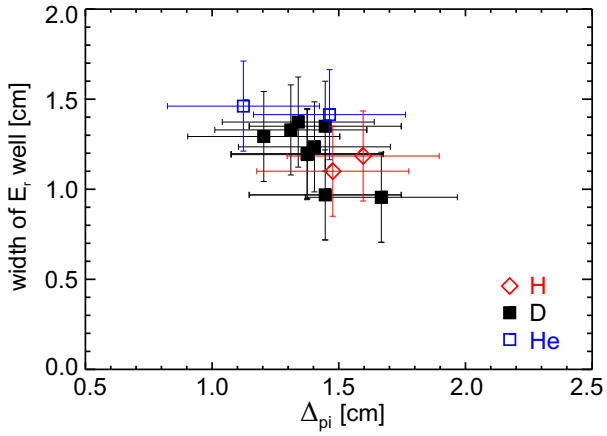

Figure 7: E_r well width plotted versus the ion pressure pedestal width.

Larmor radius $r_{L,\phi}$, which is defined as $r_{L,\phi} = \frac{\sqrt{2m_i k_B T_i}}{q_i B_\phi}$ where m_i and q_i are the mass and charge of the main ion species i and B_ϕ the toroidal magnetic field component at the pedestal top. The variations in the E_r well width are found to be small despite changing the ion temperature, magnetic field and the plasma particle species (D, H and He). A possible dependence of the E_r well width on the poloidal ion gyroradius, $r_{L,\theta} = \frac{\sqrt{2m_i k_B T_i}}{q_i B_\theta}$ with B_θ the poloidal magnetic field at the pedestal top, has been examined. The width of the E_r shear layer shows only a weak dependence on $r_{L,\theta}$ as illustrated in figure 6(c). This is consistent with observations at JFT-2M [36] and DIII-D [37] and in line with theoretical predictions of the ion orbit loss model [38, 39]. Including the effects due to orbit squeezing, it was shown analytically that in H-mode the E_r well width should be independent of the poloidal magnetic field [39].

The width of the E_r well has also been compared to the ion pressure pedestal width for a subset of discharges in which detailed n_e profiles, needed for the calculation of the ion pressure profile, were available. Here, the pedestal width of the ion pressure, Δ_{pi}, is defined as the distance between the radial position of the minimum curvature in the ion pressure profile and the separatrix and is determined in real space coordinates. It should be noted that the actual ion pedestal width could be larger since the CXRS measurements, which provide the T_i profile, are limited to the confined plasma region [12]. Figure 7 shows the width of the E_r well plotted versus the ion pedestal width. The data shows no significant dependence and indicates that for the analyzed discharges the ion pressure pedestal has an average width of 1.4 cm. This is in line with measurements in dimensionless parameter experiments at JT-60U [40], which showed a very weak dependence of the pedestal width on the main ion species. While no dependence of the ion pedestal width on the isotope is seen in the current dataset, a detailed comparison of the E_r well and the ion and electron pressure pedestal width will be performed in future dimensionless scaling experiments at AUG in which ν_* and β are matched.

Combining the data from AUG with data from other machines supports the scaling of the E_r well width with the size of the machine [6]. Figure 8 shows the average width

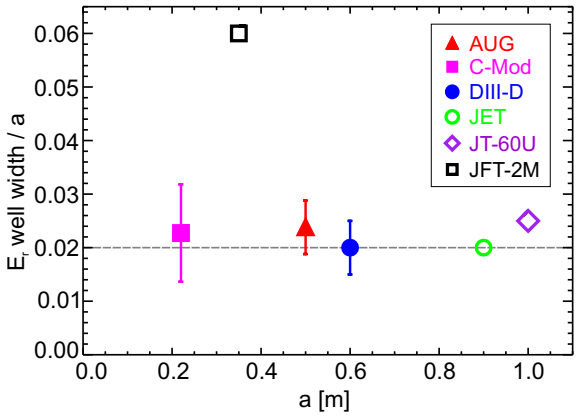

Figure 8: Multi-machine comparison: width of the E_r well, normalized to the minor radius a of the machine (data from C-Mod, DIII-D, JET, JT-60U and JFT-2M are taken from [6], [34, 35], [4], [42] and [41]), plotted as a function of the minor radius.

of the E_r well normalized to the minor radius a at AUG in comparison with E_r well widths from Alcator C-Mod [6], DIII-D [34, 35], JET [4], JFT-2M [41] and JT-60U [42]. For JT-60U, the average width for H-mode plasmas with co-injected NBI is shown. However, it should be noted that at JT-60U the E_r well width is observed to decrease when comparing co-injection to balanced- and counter-injected NBI [42]. As shown in figure 8 the data points from AUG, Alcator C-Mod, DIII-D, JET and JT-60U support the machine size scaling while the data from JFT-2M differs by a factor of 3, which might be explained by the uncertainty of the diagnostic technique as a combination of passive and active views in different toroidal sectors were employed.
At DIII-D [34] and Alcator C-Mod [6] the width of the E_r well did not vary significantly despite changing the plasma parameters, such as plasma current, magnetic field, temperature and density. The normalized toroidal Larmor radius $\rho_{*,\phi}$ varied from 3.0–6.2 at AUG, 3.2–5.3 at Alcator C-Mod [6], 4.9–9.9 at DIII-D [34, 35], 1.4 at JET [4], 7.3 at JFT-2M [41] and 3.0 at JT-60U [42]. The values for $\rho_{*,\phi}$ were evaluated using the published data from these machines.
The data from AUG, Alcator C-Mod, DIII-D, JET and JT-60U suggest that, independently of the size of the machine, the width of the E_r well corresponds to $\sim$2 % of the minor radius. Using this scaling, the width of the E_r well in ITER (with a minor radius of 2 m [43]) is estimated to 4 cm.

5. Summary and Discussion

Studies on the parameter dependence of the radial electric field have been carried out in the edge pedestal of hydrogen, deuterium and helium plasmas at AUG. Comparing the spatial structure of the E_r well to the pedestal height shows that the depth of the E_r well is correlated with the ion pressure at the pedestal top. This result is consistent with the main ion pressure gradient term $\nabla p_i/en_i$ being in balance with the edge radial

electric field. The relationship between E_r and $\nabla p_i/en_i$ is also fulfilled at the high-field side, despite the presence of a poloidal impurity density asymmetry in the edge pedestal [23, 24].

Analyzing the radial position of the E_r minimum shows that for deeper E_r wells the minimum appears to move towards the separatrix. A comparison to the radial position of the minimum in $\nabla p_i/en_i$ shows good agreement, thus suggesting that the radial distance between the steepest gradients in T_i and n_i decreases as E_r gets deeper. This is in line with the observation that the pedestal widths in the electron temperature and density are different [33] and could point to a different influence of the E_r shear on heat and particle transport. One example that manifests this behaviour is the I-mode regime [44, 45].

The width of the E_r well shows no strong dependence on the toroidal and poloidal Larmor radius and is on average 1.2 cm at AUG. This is consistent with observations at JT-60U [40] which showed that the pedestal width has only a very weak dependence on the plasma particle species. Comparison of the AUG measurements to the data from multiple machines, including Alcator C-Mod [6], DIII-D [34, 35], JET [4] and JT-60U [42], support the machine size scaling of the E_r width observed in [6] (with the exception of JFT-2M [41]; here the data shows a difference by a factor of 3 which might arise due to the uncertainty of the diagnostic technique). The data indicate that the E_r width matches $\sim$2 % of the minor radius independently of the size of the machine. This implies that in ITER the E_r well should be 4 cm wide.

In the pedestal of highly collisional H-mode plasmas the E_r well is observed to be neoclassical [16, 17], i.e. to be sustained by the gradients of the main ions. Thus, one would expect that the pedestal width in the ion pressure should also scale with the size of the machine. The open question remains what sets the pedestal width. Based on MHD stability, the EPED model [46] predicts that the pedestal width, in normalized poloidal flux, scales with the square root of $\beta_\theta^{ped,top}$, defined as the ratio between the kinetic pressure and the poloidal magnetic pressure at the pedestal top, and thus, it increases with machine size. However, recent observations [14] combining data from AUG, DIII-D and JET showed that the electron pressure pedestal width, evaluated in real space coordinates, is the same for all three machines ($\sim$1.5 cm) and therefore independent of the size of the machine. At high collision rates, the electrons and ions are sufficiently coupled such that $T_e \approx T_i$ [14] and hence, the same behaviour for the ion pressure pedestal width is expected. At low collisionality, which is targeted at ITER, the electron and ion heat channels might decouple at the plasma edge. This finding, coupled with a large variation in the ratio of the pedestal top ion temperature to the ion temperature gradient [14], suggests that the pedestal width of T_i is larger in this low collisionality regime. Note also that the gas puff has an influence on the pedestal width; at higher gas puff rates, the pedestal top value of the electron density is increased while the gradient remains the same [14]. This, in turn, also affects the width of the main ion pressure gradient term $\nabla p_i/en_i$. A detailed, multi-machine study of the ion temperature, density and pressure pedestal is required to examine the relation between

the E_r well width and the ion pedestal width and to get a better understanding of the pedestal in current and future fusion devices.
In conclusion, the results presented in this paper underline that in the H-mode pedestal the nature of E_r is neoclassical [16, 17], in accordance with early theoretical predictions [18, 19]. The measurements corroborate that the minimum of the E_r well is approximately equal to the maximum of the main ion pressure gradient term.

Acknowledgments

The first author would like to thank F. Ryter and P. Schneider for fruitful discussions and the referees for their valuable input.

References

[1] F. Wagner *et al. Phys. Rev. Lett.*, 49(19):1408, 1982.
[2] H. Biglari *et al. Phys. Fluids B*, 2:1, 1990.
[3] K. H. Burrell *et al. Phys. Plasmas*, 1(5):1536, 1994.
[4] N. Hawkes *et al. Plasma Phys. Control. Fusion*, 38:1261, 1996.
[5] J. Schirmer *et al. Nucl. Fusion*, 46:S780–S791, 2006.
[6] R. M. McDermott *et al. Phys. Plasmas*, 16:056103, 2009.
[7] K. Kamiya *et al. Nucl. Fusion*, 51:053009, 2011.
[8] E. Viezzer *et al. Nucl. Fusion*, 53:053005, 2013.
[9] S.-I. Itoh and K. Itoh. *Phys. Rev. Lett.*, 60:2276, 1988.
[10] K. Ida. *Plasma Phys. Control. Fusion*, 40:1429, 1998.
[11] G. D. Conway *et al. Plasma Fus. Research*, 5(S2005), 2010.
[12] E. Viezzer *et al. Rev. Sci. Instrum.*, 83:103501, 2012.
[13] R. J. Fonck *et al. Phys. Rev. A*, 29(6), 1984.
[14] P. A. Schneider *et al. Nucl. Fusion*, 53:073039, 2013.
[15] J. Neuhauser *et al. Plasma Phys. Control. Fusion*, 44:855, 2002.
[16] E. Viezzer *et al. Nucl. Fusion*, 54:012003, 2014.
[17] U. Stroth *et al. Plasma Phys. Control. Fusion*, 53:024006, 2011.
[18] V. Rozhansky and M. Tendler. *Phys. Fluids B*, 4:1887, 1992.
[19] V. Rozhansky and M. Tendler. *Plasma Rotation In Tokamaks.* Reviews of Plasma Physics 19, Edited by B. B. Kadomtsev, ISBN 0-306-11009-1, Plenum Publishing Corporation, New York, 1996.
[20] V. Rozhansky. *Plasma Phys. Control. Fusion*, 46:A1, 2004.
[21] T. Pütterich *et al. Nucl. Fusion*, 52:083013, 2012.
[22] R. M. Churchill *et al. Rev. Sci. Instrum.*, 84:093505, 2013.
[23] E. Viezzer *et al. Plasma Phys. Control. Fusion*, 55:124037, 2013.
[24] R. M. Churchill *et al. Nucl. Fusion*, 53:122002, 2013.
[25] T. Fülop and P. Helander. *Phys. Plasmas*, 8:3305, 2001.
[26] P. Helander and D. J. Sigmar. *Collisional Transport in Magnetized Plasmas.* 1^{st} edition, ISBN 0-521-80798 -0, Cambridge University Press, Cambridge, 2002.
[27] G. D. Conway *et al. Phys. Rev. Lett.*, 106:065001, 2011.
[28] T. S. Hahm and K. H. Burrell. *Phys. Plasmas*, 2(5):1648, 1995.
[29] G. D. Conway *et al. Plasma Phys. Control. Fusion*, 46:951, 2004.
[30] K. Kamiya *et al. Phys. Rev. Lett.*, 105:045004, 2010.
[31] P. Lang *et al. Conf. Proc. of the 24^{th} IAEA Fusion Energy Conf., EX/P4-01, San Diego*, 2012.

[32] S. Klenge. *Dynamik magnetisch eingeschlossener Plasmen am L-H Übergang.* PhD thesis, Universität Stuttgart, 2005.
[33] P. A. Schneider *et al. Plasma Phys. Control. Fusion*, 54:105009, 2012.
[34] P. Gohil *et al. Nucl. Fusion*, 38(1):93, 1998.
[35] K. H. Burrell *et al. Plasma Phys. Control. Fusion*, 46:A165, 2004.
[36] K. Ida *et al. Plasma Phys. Control. Fusion*, 36:A279, 1994.
[37] R. J. Groebner *et al. Conf. Proc. of the 13th International Conference on Plasma Physics and Controlled Nuclear Fusion Research, Vol. 1, p. 453, IAEA-CN-53/A-VI-4, Washington, DC*, 1990.
[38] K. C. Shaing and E. C. Crume, Jr. *Phys. Rev. Lett.*, 63(21):2369, 1989.
[39] K. C. Shaing. *Phys. Fluids B*, 4(2):290, 1991.
[40] H. Urano *et al. Nucl. Fusion*, 48:045008, 2008.
[41] K. Ida *et al. Phys. Rev. Lett.*, 65(11):1364, 1990.
[42] K. Kamiya *et al. Nucl. Fusion*, 52:114010, 2012.
[43] ITER. http://www.iter.org.
[44] F. Ryter *et al. Plasma Phys. Control. Fusion*, 40:725, 1998.
[45] D. G. Whyte *et al. Nucl. Fusion*, 50(105005), 2010.
[46] P. B. Snyder *et al. Nucl. Fusion*, 51:103016, 2011.